Journal of Structural Chemistry. Vol. 50, No. 1, pp. 67-77, 2009

NQR AND NMR STUDY OF HYDROGEN BONDING INTERACTIONS IN ANHYDROUS AND MONOHYDRATED GUANINE CLUSTER MODEL: A COMPUTATIONAL STUDY

M. Monajjemi, B. Honarparvar, S. M. Nasseri, and M. Khaleghian

UDC 541.571.9;543.429.2

In this paper extensive systematic computational study has been carried out to justify hydrogen bonding interactions and their influence on the oxygen, nitrogen and hydrogen NQR and NMR parameters of the anhydrous and monohydrated guanine crystal structures at two different levels, B3LYP and MP2, using 6-311++G** and D95** basis sets. These theoretical data have been compared with experimental NMR and NQR measurements. For further investigation, results of cluster calculation have been compared with that of a single molecule. Our theoretical NQR and NMR parameters of ^{17}O, ^{15}N and ^{2}H atoms of anhydrous and monohydrated guanine exhibited extreme sensitivity to electron distribution around mentioned nuclei caused by cooperative influences of various types of hydrogen bonding interactions. Fortunately, our calculated isotropic shielding values and CS tensors for the ^{17}O and ^{15}N nuclei as well as obtained ^{14}N-NQR parameters are in excellent agreement with experimental data. Therefore, we can undoubtedly conclude that for anhydrous and monohydrated guanine tetrameric clusters including intermolecular interactions, our theoretical estimates are in better agreement with observed experimental values than those in which these interactions have been ignored.

Keywords: nuclear magnetic resonance, nuclear quadrupole resonance, hydrogen bonding interactions, *ab initio*, density functional theory, DFT.

INTRODUCTION

The crystal structure of guanine is of great importance in both DNA and RNA research. Guanine nucleotides are involved in intermediary metabolism and animal tissues.The structure of single guanine molecule is essentially planar and, in contrast with guanine monohydrate, the two protonated ring nitrogen atoms are found to be N_1 and N_7 [1].

Guanine monohydrate also forms sheets, but the water molecules are incorporated in the hydrogen bonding network and promote the transfer of hydrogen atom from N_7 to N_9 in order to give favorable hydrogen bonding interactions and then represent a proper model to test the performance of quantum chemical calculations in handling hydrogen-bonding medium [2]. Considering the presence of various kinds of hydrogen bonding in the calculations, the most probable interacting molecules with the central molecule in the crystal structures of anhydrous and monohydrated guanine were found to be in the turmeric clusters (see Fig. 1).

Science and Research Branch, Islamic Azad University, P.O. Box 14515-775, Tehran, Iran; m_monajjemi@yahoo.com. The text was submitted by the authors in English. *Zhurnal Strukturnoi Khimii*, Vol. 50, No. 1, pp. 73-83, January-February, 2009. Original article submitted April, 22, 2008.

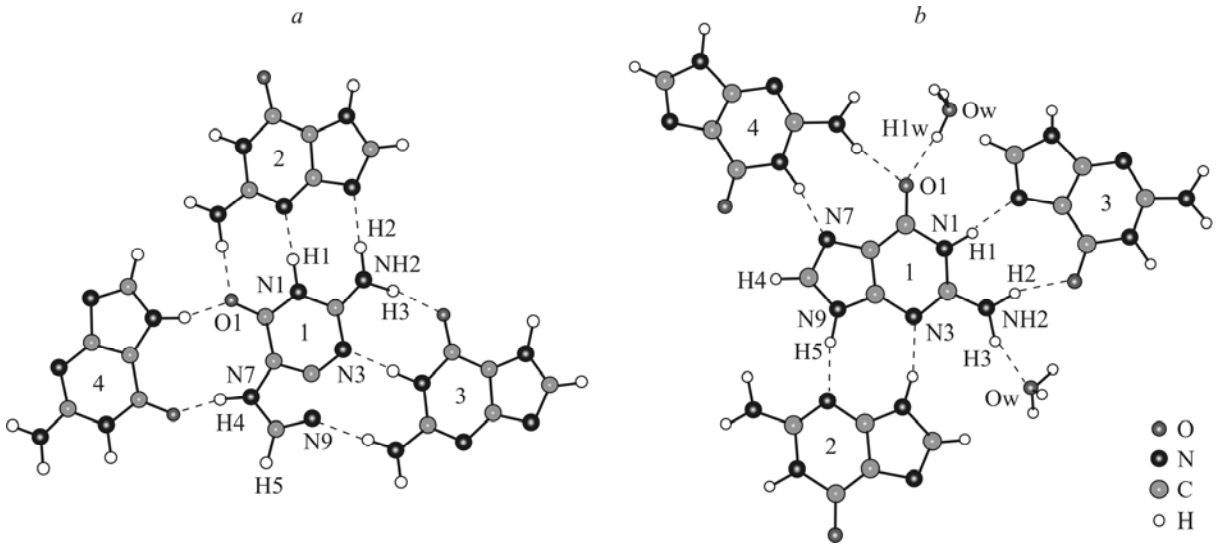

Fig. 1. Intermolecular hydrogen bonding interactions in crystalline anhydrous (*a*) and monohydrated (*b*) guanine.

Infrared absorption spectra have been studied for matrix isolated guanine and 9-methyl guanine, which is a formal analogue of the natural nucleoside in DNA and RNA [3]. Also, several reliable theoretical calculations have been performed on the ground state properties and vertical electronic transitions of guanine [4-6]. The ^{14}N-NQR frequencies, quadrupole coupling constants, and asymmetry parameters obtained from the ^{14}N-NQR spectra of the enol form of guanine have been reported experimentally by ^{14}N-proton double resonance technique involving multiple proton-nitrogen level crossing and spin mixing in the laboratory frame at 77 K [7].

In addition, for the crystal structure of guanine monohydrate, magic-angle-spinning (MAS) and static ^{17}O-NMR spectra have been acquired at 11.75 T [8].

Despite the fact that oxygen is also an abundant element in nucleic acid molecules, only few studies can be found in the literature that employ ^{17}O ($I = 5/2$) and ^{14}N ($I = 1$) NMR to investigate molecules related to nucleic acids. The lack of experimental ^{17}O and ^{15}N-NMR data is a direct consequence of the fact that it is intrinsically difficult to obtain high-resolution NMR spectra for quadrupole nuclei [8].

Therefore, it is clear that the combination of nuclear magnetic resonance (NMR) and nuclear quadrupole resonance (NQR) spectroscopies dealing with electron distributions around nuclei seem to be a versatile technique for studying structural chemistry of nucleic acid and provides logical justification of the observed results that has not been much explored yet theoretically.

It is understood that experimental studies are essential in the determination of hydrogen bonding properties, but combining them with systematic computational approaches leads to a better identification of our obtained theoretical approximations. In spite of numerous computational NMR and NQR studies, there is still a lack of systematic studies of guanine according to several monographs and review articles [9-11].

In our study, the keto-7H form of the guanine molecule has been considered which has been found to be comparable in stability with the keto-9H form and also its experimental data are available [5].

As a first step to complete account of computational solid-state NMR, we have carried out two sets of theoretical NMR calculations for anhydrous and monohydrated guanine at the level of B3LYP theory using 6-311++G** and D95** basis sets. Our main goal was focused on producing the first set of fundamental NMR tensors for mentioned crystal structures to evaluate the cooperative influence of intermolecular hydrogen-bonding interactions on these parameters.

Second, we have determined the ^{17}O, ^{14}N and ^{2}H electric field gradient (EFG tensors) of anhydrous and monohydrated guanine. For further investigation on hydrogen bonding influence on the oxygen, nitrogen and hydrogen atoms, NMR as well as EFG tensors have been calculated for both forms of the monomer and turmeric cluster model and then

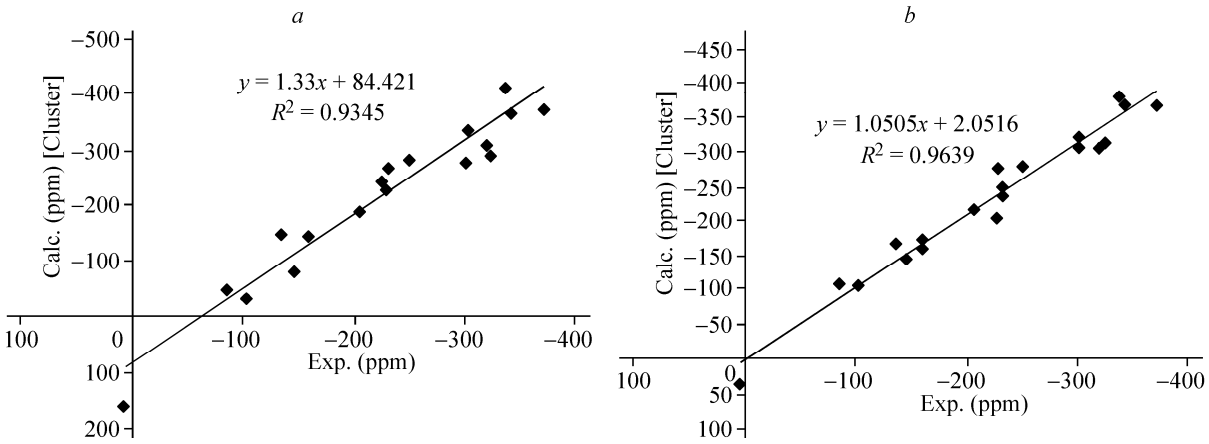

Fig. 2. Comparison of experimental and theoretical ^{15}N-NMR tensors of guanine monohydrate. (*a*) Monomer. (*b*) Cluster.

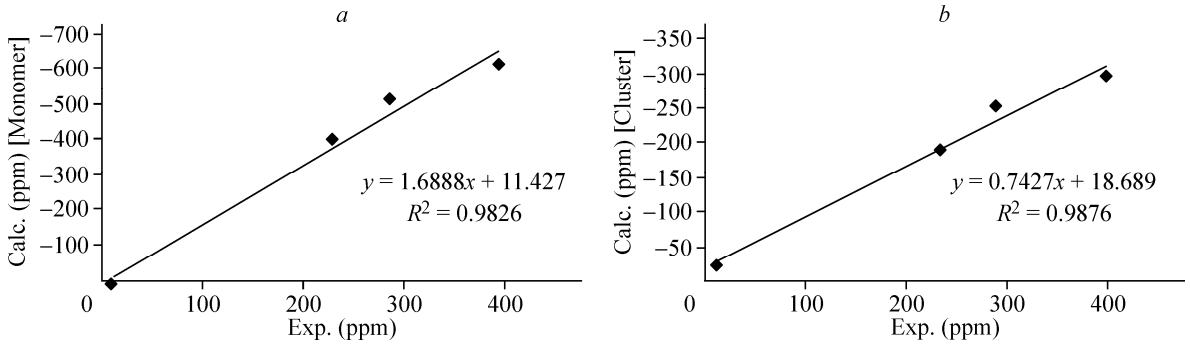

Fig. 3. Comparison of experimental and theoretical ^{17}O-NMR tensors of guanine monohydrate. (*a*) Monomer. (*b*) Cluster.

the EFG tensors converted into NQR parameters such as C_Q and η_Q. In this way, we have compared our observed experimental NQR and NMR parameters through evaluating the plotted graphs of the experimental data versus theoretical values for both oxygen and nitrogen nuclei of monomer and turmeric clusters of guanine anhydrous and monohydrated guanine (Figures 2 and 3) [7, 8].

COMPUTATIONAL DETAILS

Typically, considering computational limitations, GIAO chemical shielding calculations as implemented in G98 program need several hours of CPU time for isolated molecules and several days for large molecular clusters.

For the quadrupole interaction, molecular constants called nuclear quadrupole coupling constants depends on the quadrupole moment of the nucleus and the second derivatives of the electrostatic potential due to all molecular charges outside the nucleus (QCC), C_Q, in MHz:

$$C_Q[\text{MHz}] = e^2Qq/h, \tag{1}$$

where Q is the nuclear quadrupole moment of the nucleus. Another important parameter in the measurement of the EFG tensors deviation from axial symmetry known as the asymmetry parameter (η_Q) which can be defined by [12, 13]:

$$\eta_Q = (q_{xx} - q_{yy})/q_{zz}. \tag{2}$$

All extensive *ab initio* calculations on ^{17}O, ^{14}N and ^{2}H-EFG and isotropic chemical shielding (σ_{iso}) as well as CS tensors (σ_{ii}) for the anhydrous and monohydrates guanine were carried out using Gaussian 98 program [14].

In each step experimental data have been compared with our computational results. It should be remembered that, with our limited computing resources, long computational times were generally required for the quantum chemical calculations.

The 3-21G basis set considered all the atoms except the atoms involved in hydrogen bonding for which the 6-311++G**(*d*,*p*) and the basis set of Dunning Housing double-ξ including polarization functions, D95**, were employed [17]. The gauge including atomic orbital (GIAO) approach as implemented in G98 was applied for chemical shielding calculations [18].

The experimental geometry of crystal structures of anhydrous and monohydrated guanine obtained from X-ray diffraction studies was considered. Of course, this technique did not identified any accurate locations for hydrogen atoms; a geometry optimization of the hydrogen atoms have been performed at the B3LYP/6-311++G*** level, where during this optimization the positions of the hydrogen atoms were kept fixed. For both anhydrous and monohydrated crystalline guanine structure tetrameric clusters involving the most probable interaction molecules with the central molecule were created using coordinates transformation and were considered in the calculations of NMR and NQR parameters**.** In order to calculate the ^{17}O, ^{14}N and ^{2}H EFG tensors, the B3LYP exchange functional and MP2 levels of theory were employed [18, 19].

For further investigation on the ability of various nuclei to contribute to hydrogen bonding, all the calculations were performed for both forms of the monomer and the tetrameric cluster of anhydrous and monohydrated guanine.

RESULTS AND DISCUSSION

In this section of our paper we discuss NQR and NMR parameters of oxygen, nitrogen and hydrogen atoms of anhydrous and monohydrated tetrameric clusters in three separate sections to investigate the hydrogen bonding effects on the structure and electron distribution around these nuclei to compare the tendency of various nuclei in contributing to hydrogen bonding. The results of both B3LYP and MP2 methods using 6-311++G** and D95** basis sets are reported and discussed in details.

STRUCTURAL FEATURES

According to the crystallographic data for anhydrous and monohydrated guanine, we can realize some unique features of these compounds. The guanine molecules are connected by N–H…O (2.93 Å) and O–H…O (2.71 Å) hydrogen bonds in the tetrameric crystal structure, see Fig. 1, which is in accordance with the values for guanine monohydrate observed before [18]. The oxygen atom, O_6, also takes part in O…H–O hydrogen bond (2.71 Å) to a water molecule. In addition, each water molecule forms a hydrogen bond with NH_2 group. The C=O bond length at O_6, 1.239 Å, is close to those found for the C=O groups involved in strong hydrogen bonding [1, 2].

Intermolecular hydrogen bonding distances (Å) in both anhydrous guanine and guanine monohydrate are given in Table 1. The geometries in both cases exhibit a typical behavior of hydrogen bonded systems. This chemical behavior is confirmed by either the experimental data or *ab initio* calculations.

Due to considerable shifting of atoms appeared while going from anhydrous guanine to guanine monohydrate, no more comparison can be made in detail among these structural geometries. However, according to the data listed in Table 1, it can be seen that for guanine monohydrate the distance O1–1…N (NH_2) is longer than in anhydrous guanine which is related to hydrogen bonding effect.

INVESTIGATION OF ^{17}O, ^{15}N, AND ^{1}H-NMR PARAMETERS

NMR parameters are very useful in determining the hydrogen bonding properties and are among the most common techniques for our purpose. Experimental solid-state ^{17}O and ^{15}N-NMR data for guanine monohydrate have been reported in

TABLE 1. Intermolecular Hydrogen-Bonding Distances (Å) in Guanine Anhydrous and Monohydrate

r [target…neighbor]				r [target…neighbor]			
Anhydrous guanine		Monohydrated guanine		Anhydrous guanine		Monohydrated guanine	
H1-1…N3-2	1.857	O1-1…H1w	1.618	N1-1…N3-2	2.860	H2-1…O1-3	1.936
H2-1…N9-2	1.992	O1-1…Ow	2.710	$N_{(NH_2)}$-1…N9-2	3.006	H3-1…Ow	2.150
O1-1…H3-2	1.876	O1-1…H2-4	1.992	$N_{(NH_2)}$-1…O1-3	2.902	N3-1…N9-2	2.893
O1-1…H4-4	1.749	O1-1…$N_{(NH_2)}$-4	2.934	N3-1…N1-3	2.861	N3-1…H5-2	1.877
H4-1…O1-4	1.746	N1-1…N7-3	2.839	N9-1… $N_{(NH_2)}$-3	3.006	N9-1…N3-2	2.892
H3-1…O1-3	1.875	H1-1…N7-3	1.801	N7-1…O1-4	2.742	H5-1…N3-2	1.864
N3-1…H1-3	1.856	$N_{(NH_2)}$-1…O1-3	2.934	O1-1… $N_{(NH_2)}$-2	2.902	N7-1…N1-4	2.841
N9-1…H2-3	1.991	$N_{(NH_2)}$-1…Ow	2.992	O1-1…N7-4	2.743	N7-1…H1-4	1.817

TABLE 2. Calculated ^{15}N and ^{17}O and H–CS Tensors of Guanine Anhydrous Using 6-31++G** and D95** Basis Sets

Nuclei	σ_{ii}	Monomer	Cluster	Monomer	Cluster
N_1	σ_{11}	–154	–170		
		(–164)	(–154)	(–242)	–245
	σ_{22}	–270	–25		–236
		(–277)	(–245)		(233)
	σ_{33}	–282	306		
		(–286)	(–287)		
NH_2	σ_{11}	–276	–250		
		(–290)	(–249)	–320	–305
	σ_{22}	–297	–322	(–326)	(–299)
		(–306)	(–316)		
	σ_{33}	–386	–342		
		(–381)	(–333)		
N_3	σ_{11}	–34	–104		
		(–62)	(–88)	–179	–216
	σ_{22}	–132	–169	(–196)	(–205)
		(–148)	(–161)		
	σ_{33}	–371	–376		
		(–377)	(–366)		
N_7	σ_{11}	–138	–145	–239	–239
		(_153)	(–133)	(–231)	(–231)
	σ_{22}	–265	–245		
		(–273)	(–238)		
	σ_{33}	–315	–327		
		(–324)	(–322)		
N_9	σ_{11}	83	–10		
		(58)	(9)	–104	–154
	σ_{22}	–52	–105	(–123)	(–144)
		(_62)	(92)		
	σ_{33}	–345	–357		
		(–358)	(–350)		
O	σ_{11}	565	365		
		(561)	(390)	329	222
	σ_{22}	433	290	(317)	(238)
		(415)	(310)		
	σ_{33}	–10	6		
		(–24)	(13)		
H_2	σ_{11}	22	8	28	22
		(21)	(9)	(28)	(22)
	σ_{22}	27	21		
		(27)	(21)		
	σ_{33}	35	35		
		(35)	(36)		
H_3	σ_{11}	21	8	27	21
		(21)	(8)	(27)	(21)
	σ_{22}	25	19		
		(25)	(20)		
	σ_{33}	35	36		
		(35)	(36)		
H_4	σ_{11}	18	4		
		(17)	(4)	23	17
		24	16	(23)	(17)
		(23)	(16)		
		28	31		
		(28)	(31)		

molecular cluster models where a complete hydrogen bonding network has been considered [8, 19]. However, there are no experimental data of solid-state ^{17}O-NMR for anhydrous guanine.

TABLE 3. ^{14}N and ^{17}O-EFG Tensors of Guanine Anhydrous Using I: 6-311++G** and II: D95** Basis Sets

Nucleus	Level	Monomer	Cluster	Monomer	Cluster	Experiment	
		C_Q (MHz)	C_Q (MHz)	η_Q	η_Q	C_Q (MHz)	η_Q
N_1	B3LYP/I	3.95	2.79	0.14	0.50	3.610	0.37
	MP2/I	4.28	3.26	0.13	0.46		
	B3LYP/II	4.15	3.35	0.14	0.48		
NH_2	MP2/II	4.66	3.23	0.12	0.45		
	B3LYP/I	5.09	3.38	0.12	0.48	3.480	0.38
	MP2/I	5.28	3.72	0.13	0.47		
N_3	B3LYP/II	5.33	3.90	0.14	0.49		
	MP2/II	5.67	3.98	0.14	0.46		
	B3LYP/I	3.32	2.68	0.81	0.91	3.300	0.38
	MP2/I	3.42	3.12	0.97	0.70		
N_7	B3LYP/II	3.15	3.16	0.99	0.70		
	MP2/II	3.64	3.42	0.83	0.98		
	B3LYP/I	3.07	2.07	0.11	0.60	1.730	0.15
	MP2/I	3.27	2.30	0.05	0.59		
N_9	B3LYP/II	3.35	1.99	0.09	0.53		
	MP2/II	3.66	3.40	0.03	0.55		
	B3LYP/I	4.08	3.21	0.08	0.26	0.096	0.08
	MP2/I	4.31	3.45	0.14	0.353		
	B3LYP/II	3.84	3.35	0.21	0.44		
	MP2/II	4.18	3.12	0.27	0.47		
O_1	B3LYP/I	9.11	6.94	0.41	0.86	—	—
	B3YP/II	9.28	7.52	0.49	0.98	—	—
	MP2/I	9.71	7.54	0.49	0.92	—	—
	MP2/II	10.08	5.57	0.57	0.87	—	—

In this section of our study, we report a complete theoretical discussion of solid state tensors of ^{17}O, ^{15}N and ^{1}H nuclei of anhydrous and monohydrated guanine which are summarized in Tables 2 and 3.

From the theoretical results presented in Table 3 for monohydrated guanine, many important facts can be realized. For oxygen atom which forms two hydrogen bonds and plays an important role in enhancing the hydrogen-bonding effect, the experimental isotropic shielding is found to be about 230 ppm that is closer to cluster form rather than the monomeric state and the obtained results demonstrate a remarkable improvement. In other words, when a single molecule is considered, computed CS tensor components deviate significantly from the observed values for the crystal structure. In each case, the largest deviation occurred with σ_{11} components.

It is interesting to note that employing B3LYP/ D95** level of theory proved to be more appropriate computational model for the prediction of the ^{17}O-isotropic shielding in monohydrated guanine (193 ppm). Of course, the theoretical values obtained under the experimental data, revealed that calculations at the B3LYP/ D95** level of theory underestimate the ^{17}O-isotropic shielding by about 4 ppm.

Furthermore, both theoretical and experimental observations confirmed the significant decreasing trend of ^{17}O-isotropic shielding (increase in paramagnetic shielding) on going from monomer down to tetrameric cluster model. This decreasing trend reveals the key role of oxygen atom in contributing to the hydrogen bonding in the crystalline monohydrated guanine. This is consistent with the expectation that the crystal lattice represents an environment where hydrogen bonding is the strongest.

About the CS tensor components, an important fact that can be found out from Tables 2 and 3 is that σ_{ii} show even wider variations than do the isotropic chemical shifts σ_{iso}. Similarly, regarding both theory and experiment, the same trend has been observed for these values, i.e. decreasing trend can be seen on going from monomer down to cluster, except for σ_{33} which yielded negative values for the monomer and lower values than cluster. In each case the results correspond to the cluster model are closer to experimental data. Therefore, we can strongly conclude that to investigate the hydrogen bonding influence considering crystal structures reveal reliable results that are in better agreement with the experiment where a complete hydrogen bonding network is considered. Clearly, inclusion of several immediate neighbor molecules in the theoretical model can reproduce, to a very good degree of accuracy, the ^{17}O-NMR properties in the crystal lattice.

Accordingly, on the basis of computed results, in some cases CS tensor components reveal significant sensitivity to the basis set. Choosing D95** basis set especially for the $\sigma_{33}^{theor} = \sigma_{33}^{exp} = 10$ ppm, seems to yield results closer to the experimental data. Also, for the σ_{11}, through employing D95** basis set the $\sigma_{11}^{theor} = 319$ ppm obtained about 20 ppm closer to the observed value ($\sigma_{11}^{exp} = 319$ ppm) in the experiment. In fact, the water molecule is a strong hydrogen bond donor, which may contribute significantly to the values and δ_{iso} and σ_{ii}.

As it is expected, NMR parameters of all five nitrogen atoms with different chemical environment obtained are different and have negative values. However, theory predicted an exception for σ_{11} of N_7 which has positive value (6 ppm) that reveals its shielding position as compared with other nitrogen atoms. We should emphasize that these σ values are being shifted with respect to the single molecule. Positive values indicate diamagnetic or lower frequency shifts; more negative values are related to paramagnetic or higher frequency shifts. In this case, due to the hydrogen bonding formation, decreasing trend obtained for monomer as compared with monohydrated cluster, but the result (71 ppm) was very far from the observed value (6 ppm) [21, 22]. Another striking feature is that we encountered more negative values while passing from monomer to cluster. Again, according to Tables 2 and 3 we can see some exceptions for σ_{22}, σ_{33}, and σ_{iso} of NH_2, σ_{22}, σ_{33} of N_3 and σ_{22} of N_9 whose less negative values can be understood due to the hydrogen bonding interactions. Here we may clearly realize an important fact that among CS tensors variations in σ_{22} and σ_{33} components of a given nucleus are more responsible for the observed hydrogen bonding effects.

The same result as for oxygen atom is true while comparing our nitrogen data with the experimental observations; i.e., assuming the crystal structure using D95** basis set, a satisfactory agreement is indeed observed with the experimental data. For instance, σ_{iso} (N_1), σ_{iso} (N_3), and σ_{22} (NH_2) exhibit insignificant difference (about 1 ppm) with the experiment. However, in two cases such as $\sigma_{33}^{cluster}(NH_2) = -380$ ppm and $\sigma_{iso}^{cluster}(NH_2) = -380$ ppm, no basis set effect has been observed; i.e., the results of both 6-311++G** and D95** basis sets are the same.

As also seen in Figures 2 and 3 which display the graphs of the ^{17}O and ^{15}N-NMR experimental data versus their theoretical values, for each of the monomer and tetramer cluster forms the experimental correlation is very well reproduced by the density functional coincidence. However, it should be noted that even though the two plotted graphs have fundamentally very close slopes, comparing these two slopes in Figs. 2 and 3 reveals an important implication that the case considering cluster form produces a slope of 1.050 for nitrogen and 0.742 for oxygen that reveal better agreement with the experiment. Interestingly, the two sets of plotted graphs yielded nearly identical orientations for the ^{17}O and ^{15}N-NMR tensors of guanine monohydrate.

The comparison of both experimental and theoretical results of σ_{iso} parameters for the nitrogen atoms with one another can lead us to a general trend as below:

$$\sigma_{iso}(NH_2) < \sigma_{iso}(N_1H) < \sigma_{iso}(N_9H) < \sigma_{iso}(N_3) < \sigma_{iso}(N_7).$$

In order to justify the above trend, we can first refer to the ability of the two hydrogen bonds of NH_2 group with the oxygen atom of water and the oxygen atom of neighboring guanine molecules which may cause shielding on the nitrogen atom and then yield the most negative value of σ_{iso}. The same reasoning can be applied for the protonated nitrogen atoms of

the crystal structure of the guanine monohydrate (N_1H and N_9H) which behave as proton donors demonstrating significant intermolecular effects.

It may be noted that for nonprotonated nitrogen atoms, which act as proton acceptors, the hydrogen bonding effects leaded to less negative value of σ_{iso}.

In addition, hybridization of *p*-orbital with *s*-orbital also increases the shielding on the nucleus and then leads to a more negative value of σ_{iso}. Here, NH_2 group has sp^3 hybridization while N_1H and N_9H have sp^2 and N_3, N_7 exhibit *sp* hybridization. Therefore, according to the two mentioned factors, our observed trend seems to be logical and acceptable.

As a whole, the agreement between theory and experiment is sufficiently good, providing some confidence in the predicted NMR parameters for the other compounds. Nevertheless, it is important to point out that due to the complex nature of hydrogen bonding interactions, neither the CS tensor components nor isotropic chemical shifts σ_{iso} alone can provide an adequate clarification of the observed trends in NMR tensors. Further work is clearly needed to provide a unified theory for studying structural features of these cluster compounds.

To the best of our knowledge, there are no experimental NMR data for the hydrogen atoms. However, to acquire more structural information it would be of interest to compare our theoretical results with those obtained from crystallographic data. Regarding to Table 3 for ^{1}H-CS tensors of guanine monohydrated, much smaller ^{1}H-CS tensor have been obtained for the cluster form than those found for the monomer one except for H_2 atom which is connected to the oxygen atom of guanine molecule (see Fig. 1).

Furthermore, as seen in Figure 3, hydrogen nuclei existing in the monohydrated guanine crystal structures have different contributions to the hydrogen bonding. Regarding to ref. [2], atoms H_6, H_7 and H_8 belong to water and their positions are half populated.

The comparison of the results of isotropic chemical shifts σ_{iso} presented in Tables 2 and 3 reveal different contributions of the atoms to hydrogen bonding. For instance, H_4 is the only atom without any hydrogen bonding interaction (see Fig. 1). This is why the lowest value of σ_{iso} for guanine monohydrate corresponds to this atom which is more shielded in comparison with other hydrogen atoms.

On the other hand, the largest value of σ_{iso} for H_2 atom of NH_2 group has been obtained (27 ppm). Since this atom is connected to the oxygen and nitrogen atoms which have high electronegativity, it should be more deshielded and yields the largest value of σ_{iso}.

INVESTIGATION OF NQR PARAMETERS

Due to the electrostatic characteristic of hydrogen bonding, NQR techniques dealing with electron distributions around nuclei are preferred to characterize the hydrogen bonding properties from a theoretical point of view.

The electric field gradient tensors of anhydrous guanine that converted into the NQR parameters such as C_Q and η_Q as well as experimental data are collected in Tables 4. According to our reported data, considering B3LYP and MP2 methods with 6-311++G** and D95** basis sets, we can clearly judge about the hydrogen bonding effects on these NQR parameters.

The comparison of our results of quantum mechanical calculations of the ^{14}N-NQR parameters with the experimental values measured for anhydrous guanine reveals several major facts. Both experimental and theoretical ^{14}N-NQR parameters show similar but quantitatively different trend.

First, among the different methods and basis sets used, the result of *ab initio* calculation at the level of B3LYP/6-311++G** theory in three cases yielded the least discrepancy from the experiment.

Second, based on our reported data, we see two individual groups of nitrogen atoms with contrasting chemical properties: three nitrogen atoms related to six-membered ring (N_1, N_3 in the ring and NH_2 group) and two nitrogens (N_7 and N_9) in five-membered ring of guanine.

TABLE 4. ^{2}H-EFG Tensors of Guanine Anhydrous Using I: 6-311++G** and II: D95** Basis Sets

Nuc-leus	Level	Monomer	Cluster	Monomer	Cluster	Nuc-leus	Level	Monomer	Cluster	Monomer	Cluster
		C_Q (MHz)	C_Q (MHz)	η_Q	η_Q			C_Q (MHz)	C_Q (MHz)	η_Q	η_Q
H_1	B3LYP/I	265	18	0.17	0.27	H_3	B3LYP/I	277	199	0.18	0.24
	MP2/I	263	186	0.21	0.32		MP2/I	274	201	0.21	0.27
	B3LYP/II	263	191	0.18	0.27		B3LYP/II	275	207	0.19	0.23
	MP2/II	268	195	0.21	0.25		MP2/II	279	199	0.21	0.26
H_2	B3LYP/I	284	222	0.21	0.23	H_4	B3LYP/I	272	194	0.13	0.19
	MP2/I	282	226	0.24	0.26		MP2/I	270	195	0.17	0.23
	B3LYP/II	281	230	0.22	0.23		B3LYP/II	270	199	0.14	0.18
	MP2/II	287	234	0.24	0.29		MP2/II	275	199	0.16	0.19

In other words, the three nitrogen atoms involved in six-membered ring yield C_Q which falls within the range expected for the crystal structure. This satisfactory agreement and insignificant differences, especially for N_3 (ΔC_Q = 0.1 MHz) involved directly in aromatic ring, can be attributed to both strong intermolecular effects and the resonance effects in the six-membered aromatic system, electronic charge delocalization and fused condition.

In contrast, the computed C_Q values for N_7 and N_9 of anhydrous guanine, especially for N9 (ΔC_Q = 3.104 MHz), revealed significant discrepancies from experimental data. This poor agreement presented in Table 4 is not surprising because such six-membered aromatic system allows intermolecular electron delocalization or charge transfer to appear in an extremely concerted behavior. This cooperative influence leads to much stronger hydrogen bonding interaction. At the same time, the two nitrogen atoms involved in the five-membered ring have no such condition and have tendency to be involved in more hydrogen bonding contribution. This is the main reason why these two nitrogen atoms exhibit greater deviations from the experiment.

Interestingly, in contrast to the coupling constants (C_Q), especially for N_7 ($\Delta\eta$ = 0.06), an opposite trend was found for asymmetry parameter (η) values for N_7 and N_9 atoms; i.e. less differences can be seen for asymmetry parameters of these two atoms. This theoretical evidence may refer to the different sites of protonation, N_7 versus N_9, noted before [1].

Third, according to the results listed in Table 4, considering both B3LYP and MP2 methods with two mentioned basis sets, in a similar fashion the C_Q values of nitrogen atoms decrease from the monomer down to the tetrameric cluster except for N_3 of anhydrous guanine.

Besides, the corresponding asymmetry parameters showed the opposite trend and increased from the monomer up to the higher values. Of course, there is still a good coincidence between the values of computed and experimental values. According to Tables 4, the same decreasing trend for quadrupole coupling constants and increasing trend for asymmetry parameters can be seen for ^{17}O and ^{2}H atoms.

Another comprehensive finding is that there are more possibilities for the nitrogen atom of NH_2 group to be more involved in hydrogen bonding environment. For this atom even much larger reduction and shifts of the ^{14}N-quadrupole coupling constant from the monomer to the cluster structure of anhydrous guanine has been obtained, $\Delta C_Q(^{14}N)$ = 1.71 MHz. Therefore, it is expected that its NQR parameters depend strongly on the cluster model used in the calculation. In addition, as seen from Table 4 showing the ^{17}O-EFG tensors of anhydrous guanine, for oxygen atom such a variation of the ^{17}O-NQR parameters from the monomer to the cluster is much larger than that of ^{17}O-NQR one, $\Delta C_Q(^{17}O)$ = 2.17 MHz. This result demonstrates the stronger dependence of ^{17}O-NQR parameters on the cluster model and their stronger contribution to hydrogen bonding environment in comparison with nitrogen atom.

Furthermore, since the lone-pair orbital contribution is the greatest to the C_Q values of ^{14}N nucleus, it is expected that the lone-pair character will be more pronounced in the bicoordinate nitrogen atom than in the tricoordinate one, where the lone-pair electrons is conjugated with the π-system of the ring, thus giving smaller C_Q values.

No NQR data have been reported yet for ^{17}O and ^{2}H nuclei of anhydrous guanine and for ^{14}N and ^{2}H atoms of monohydrated one. But experimental measurements for only ^{17}O-NQR parameters in guanine has been found in ref. [8]. These data are listed beside our ^{14}N, ^{2}H and ^{17}O-NQR theoretical results in Tables 4.

Again, in the case of guanine monohydrate where the whole hydrogen bonding network is considered, the quadrupole coupling constant, which has been obtained at the level of B3LYP/6-311++G** theory, reveals the least discrepancy and excellent agreement between experimental solid-state ^{17}O NMR data ($\Delta C_Q(^{17}O) = 0.33$ MHz). Even higher accuracy has been found for asymmetry parameter $\eta(^{17}O)$ of guanine monohydrate at the levels of B3LYP/D95** and MP2/6-311++G** theory ($\Delta\eta(^{17}O) = 0.02$).

In addition, comparison of our computed results for anhydrous guanine with that of monohydrate structure show that for guanine monohydrate, where the whole hydrogen bonding network is considered, the trend of increasing in both quadrupole coupling constant and asymmetry parameter is observed as compared with anhydrous form.

We should note that in many nitrogen containing compounds the monomer is non-planar, while the crystal structures show intermolecular hydrogen bonding and planarity. Thus to generate quadrupole coupling constants which can be compared with experimental solid data, the cluster form is relevant and the effects of hydrogen bonding have to be taken into account.

It should be pointed out again that the X-ray crystallographic data of the keto form of crystalline anhydrous guanine were included in the calculations, while the experimental ^{14}N-NQR observations have been performed assuming enol structure. Therefore, the observed discrepancies between calculated values and experimental parameters seem to be reasonable.

CONCLUSIONS

In the current study, the major goal is focused on the systematic investigation of NMR and NQR tensors of oxygen, nitrogen and hydrogen nuclei involving crystalline anhydrous and monohydrated guanine. The theoretical values reported in this study may be useful in future for generalizing quantum properties for such hydrogen bonded systems. Some of our informative findings can be summarized as follows:

- The experimental and theoretical results have indicated that significant shifts in both CS and EFG tensors are due to the hydrogen bonding interactions as well as electrostatic interactions. The experimental and theoretical results have indicated that, especially in guanine monohydrate, the strong hydrogen bonding interaction around the oxygen, nitrogen and hydrogen atoms is responsible for a decreasing change of isotropic shielding (σ_{iso}), CS tensors (σ_{ii}), and quadrupole coupling constants (C_Q) as well as increasing trend of asymmetry parameters (η) as compared to that of a single molecule of guanine, the change being observed at B3LYP and MP2 levels with 6-311++G** and D95** basis sets.
- Regarding significant shifts in NMR and NQR data while going from the free monomer to cluster, a direct comparison of the computed NMR and NQR parameters with experiments cannot be made. Further investigations are necessary required to achieve general understanding of the effects of intermolecular hydrogen bond on the variation of the NMR and NQR parameters in computational viewpoint.
- The comparison of our computed results for anhydrous guanine with those for the monohydrate structure show that for guanine monohydrate, where the whole hydrogen bonding network is involved, an increase in both quadrupole coupling constant and asymmetry parameter is observed.

Lone-pair character will be more pronounced in the bicoordinate nitrogen than in the tricoordinate one, where the lone-pair electrons are conjugated with the π-system of the ring, thus giving smaller C_Q and then greater η values.

REFERENCES

1. K. Guille and W. Clegg, *Acta. Crystallogr*., **C62**, o515-o517 (2006).
2. U. Thewalt, C. E. Bugg, and R. E. Marsh, *ibid*., **B27**, 2358-2363 (1971).
3. K. Szczepaniak, and M. Szczesniak, *J. Mol. Struct*., **156**, 29-42 (1987).
4. S. S. Mallajsyula, A. Datta, and S. K. Pati, *Synthetic Metals*, **155**, 398-401 (2005).
5. R. Rivelino, V. Ludwig, E. Rissi, and S. Canuto, *J. Mol. Struct*., **615**, 257-266 (2002).
6. F. Erkoc and S. Erkoc, *ibid*., **589**, 405-411 (2002).
7. R. Blinc, M. Mali, R. Osredkar, et al., *J. Chem. Phys*., **57**, 5087-5093 (1972).
8. G. Wu, S. Dong, R. Ida, and N. Reen, *J. Am. Chem. Soc*., **124**, 1768-1777 (2002).
9. M. K. Shukla, S. K. Mishra, A. Kumar, and P. C. Mishra, *J. Comp. Chem*., **21**, 826-846 (2000).
10. J. P. Kehrer, *Toxicology*, **140**, 43-50 (2000).
11. J. D. Watson and C. F. H. Crick, *Nature*, **171**, 737/738 (1953).
12. M. J. Duer, *Solid State NMR Spectroscopy: Principles, Applications*, India Press (2003).
13. J. Mason, *Multinuclear NMR,* Plenum Press, New York (1987).
14. M. J. Frisch, G. W. Trucks, H. B. Schlegel, et al., *Gaussian-98, Revision A*.7. Gaussian, Inc., Pittsburgh PA (1998).
15. E. A. C. Lucken, *Nuclear Quadrupole Coupling Constant*, Academic Press, New York (1969).
16. R. K. Harris, *Nuclear Magnetic Resonance Spectroscopy, a Physicochemical Veiw*, Pitman, London Press (1983).
17. T. H. Dunning, P. G. Hay, and H. F. Schaefer, *Modern Theoretical Chemistry*, **3**, 1, New York (1976).
18. R. E. Wasylishen, S. S. Mooibroek, and J. B. Macdonald, *J. Chem. Phys*., **81**, 1057-1059 (1984).
19. A. D. Becke, *ibid*., **98**, 5648 (1993).
20. C. Lee, W. Yang, and R. G. Parr, *Phys. Rev. B*, **37**, 785-789 (1998).
21. J. Leszczynski, *J. Phys. Chem. A*, **102**, 2357 (1998).
22. J. Z. Hu, J. C. Facelli, D. W. Alderman, et al., *J. Am. Chem. Soc*., **120**, 9863-9869 (1998).